# Investigation on the rotational bedding of king piles on the basis of model tests

IOP Conf. Series: Earth and Environmental Science **727** (2021) 012024 doi:10.1088/1755-1315/727/1/012024

# Investigation on the rotational bedding of king piles on the basis of model tests

**Jannik Beuße**

Institute of Geotechnical Engineering and Construction Management, Hamburg University of Technology, Hamburg, Germany

E-mail: jannik.beusse@tuhh.de

**Jürgen Grabe**

Institute of Geotechnical Engineering and Construction Management, Hamburg University of Technology, Hamburg, Germany

E-mail: grabe@tuhh.de

**Abstract.** Rising world trade and the following consolidation of material flows cause a growing need for bigger bulk carriers. Therefore, the quay walls of the harbours need to be adjusted to realize the depth of the channels. Combined sheet pile walls are used to build quay walls. They consist out of up to 45 m long H-shaped beams and Z-shaped intermediate piles. As a result of the loads, which cause normal forces and bending moments, the stability of the slender profiles is endangered, whereby the deflection of the profile head and the embedding in the soil plays an important role. With the introduction of the standards of DIN EN 1993-5:2010-12 [1] in connection with DIN EN 1993-1-1:2010-12 [2] the proofing of combined walls needs to be done under combination of the resistance against flexural buckling and lateral-torsional buckling. For that reason the rotational resistance of the soil must be considered in order to ensure an economical design. The rotational bedding in cohesive soil is different from that in noncohesive soil and was investigated by laboratory tests as well as by numerical simulations. The results of a FOSTA / aif project with the goal of optimizing the stability procedure of combined walls are be presented.

## 1. Introduction

Distorted king piles can lead to a failure in the connection between the king pile and the sheet pile. In contrast to the resistance of the sheet piles against rotation of the king pile, the rotational bedding of the soil has a bigger influence. Currently the calculation for combined walls is only done for the final state without taking the resistance of the soil against rotation and buckling into account. Due to the introduction of the standards of DIN EN 1993-5:2010-12 [1] in connection with DIN EN 1993-1-1:2010-12 [2] the proofing of combined walls needs to be done under combination of the resistance against flexural buckling and lateral-torsional buckling. For that reason the rotational resistance of the soil must be considered in order to ensure an economical design. The rotational bedding in cohesive soil is different from that in noncohesive soil and was investigated by laboratory tests as well as by numerical simulations. The results of a FOSTA / aif project with the goal of optimizing the stability procedure of combined walls are to be presented.

## 2. Rotational bedding as additional resistance against torsional flexural buckling

Before presenting the implementation of a rotational bedding to the calculation of king piles, the important parts of the verification against torsional flexural buckling with respect to DIN EN 1993-5:2010-12 [1] and DIN EN 1993-1-1:2010-12 [2] are presented.

### *2.1. Torsional flexural buckling of beams*

If a beam is stressed by bending around the main axis, the following verification against torsional flexural buckling is shown:

$$\frac{M_{\mathrm{Ed}}}{M_{\mathrm{b,Rd}}} = \frac{M_{\mathrm{Ed}}}{\chi_{\mathrm{LT}} \cdot W_{\mathrm{y}} \cdot f_{\mathrm{y}}/\lambda_{\mathrm{M1}}} \leq 1,0 \tag{1}$$

where $\chi_{\mathrm{LT}}$ is the reduction factor for torsional flexural buckling and is calculated as follows:

$$\chi_{\mathrm{LT}} = \frac{1}{\Phi_{\mathrm{LT}} + \sqrt{\Phi_{\mathrm{LT}}^2 - \lambda_{\mathrm{LT}}^2}} \leq 1,0 \tag{2}$$

using

$$\Phi_{\mathrm{LT}} = 0,5 \cdot [1 + \alpha_{\mathrm{LT}}(\lambda_{\mathrm{LT}} - 0,2) + \lambda_{\mathrm{LT}}^2] \tag{3}$$

and

$$\lambda_{\mathrm{LT}} = \sqrt{\frac{W_{\mathrm{y}} \cdot f_{\mathrm{y}}}{M_{\mathrm{cr}}}} \tag{4}$$

The presented reduction factor $\chi_{\mathrm{LT}}$ applies to the "general design case", according to *Section 6.3.2.2 of DIN EN 1993-1-1:2010-12* [2]. The imperfection coefficient $\alpha_{\mathrm{LT}}$ can be read from Table 6.3 [2] by determining the bending lines for torsional flexural buckling. If a beam is stressed by bending around the main axis, the following check against torsional flexural buckling is shown:

$$\frac{N_{\mathrm{Ed}}}{\chi_{\mathrm{y}} \cdot N_{Rk}/\gamma_{\mathrm{M1}}} + k_{\mathrm{yy}} \cdot \frac{M_{\mathrm{y,Ed}} + \Delta M_{\mathrm{y,Ed}}}{\chi_{\mathrm{LT}} \cdot M_{\mathrm{y,Rk}}/\gamma_{\mathrm{M1}}} + k_{\mathrm{yz}} \cdot \frac{M_{\mathrm{z,Ed}} + \Delta M_{\mathrm{z,Ed}}}{M_{\mathrm{z,Rk}}/\gamma_{\mathrm{M1}}} \leq 1,0 \tag{5}$$

respectively

$$\frac{N_{\mathrm{Ed}}}{\chi_{\mathrm{z}} \cdot N_{\mathrm{RK}}/\gamma_{\mathrm{M1}}} + k_{\mathrm{zy}} \cdot \frac{M_{\mathrm{y,Ed}} + \Delta M_{\mathrm{y,Ed}}}{\chi_{\mathrm{LT}} \cdot M_{\mathrm{y,Rk}}/\gamma_{\mathrm{M1}}} + k_{\mathrm{zz}} \cdot \frac{M_{\mathrm{z,Ed}} + \Delta M_{\mathrm{z,Ed}}}{M_{\mathrm{z,Rk}}/\gamma_{\mathrm{M1}}} \leq 1,0 \tag{6}$$

where $k_{\mathrm{yy}}, k_{\mathrm{yz}}, k_{\mathrm{zy}}$ and $k_{\mathrm{zz}}$ are interaction factors for the combination of buckling and torsion. The influence of buckling is described by the factors $\chi_{\mathrm{y}}$ and $\chi_{\mathrm{z}}$.

### *2.2. Stabilising rotational bedding of construction buildings*

To calculate the slenderness $\lambda_{\mathrm{LT}}$, the ideal torsional flexural buckling $M_{\mathrm{cr}}$ is required. According to [3], the result is for forked single-span beams with a constant double symmetrical cross-section without torsional stress and under constant normal force:

$$M_{\mathrm{cr}} = \zeta \cdot N_{\mathrm{cr,z}} \cdot (0,5 \cdot z_q + \sqrt{0,25 \cdot z_{\mathrm{q}}^2 + c^2}) \tag{7}$$

with $\zeta$ as moment coefficient according to *Table 6.14* by [3], $N_{\mathrm{cr,z}}$ as ideal buckling load, $z_{\mathrm{q}}$ as distance between load application point to the centre of gravity parallel to the z-axis and $c$ as turning radius.

The turning radius $c$ can be calculated as follows:

$$c^2 = (I_{\mathrm{w}} + 0,039 \cdot L_{\mathrm{LT}}^2 \cdot I_{\mathrm{T}})/I_{\mathrm{z}} \tag{8}$$

with $I_{\mathrm{w}}, I_{\mathrm{T}}, I_{\mathrm{z}}$ as moments of curvature, torsion and inertia about the z-axis and $L_{\mathrm{LT}}$ as distance of the fork bearings.

Stiffening elements such as adjoining components or trapezoidal sheets on purlins can be idealized by a continuously rotating spring $c_\vartheta$ or by a single spring $C_\vartheta$ [3]. An adequate torsional restraint of the component at risk of torsional flexural buckling can be verified with the following equation:

$$c_{\vartheta,k} > \frac{M_{\mathrm{pl,k}}^2}{EI_{\mathrm{z}}} \cdot K_\vartheta \cdot K_V \tag{9}$$

with $K_\vartheta$ as factor for taking the course of moments and the type of twistability of the supported beam into account, $K_{\mathrm{V}} = 0{,}35$ for the elastic calculation and 1,0 for the plastic calculation. $M_{\mathrm{pl,k}}$ is the plastic moment and $EI_{\mathrm{z}}$ is the lateral or bending stiffness around the z-axis. If the minimum rotational bedding for typical component design is not achieved, the following equation can be used. According to this equation, the existing torsional stiffness is increased by a torsional bedding dependent term:

$$I_{\mathrm{T}} = I_{\mathrm{T}} + c_\vartheta \cdot \frac{L^2}{\phi^2 \cdot G} \tag{10}$$

It is important to note that this equation is no longer suitable for high rotational bedding values or beams with a bound rotational axis, since the assumption of a half sine wave as eigenmode (on which the equation is based) is not longer valid.

*2.3. Stabilising rotational bedding for soil structures*

In geotechnical problems, there are generally no additional stiffening elements connected to beams, installed in soil. However, the soil does resist against a rotation of an installed beam. Known from vane shear tests, the shear resistance depends on the particle size distribution, the size of the profile, the consistency of the soil as well as on the stress level of the soil. For cohesive soils, there is an additional influence by the velocity because of the rate dependent stress strain behaviour. Therefore, approaches for the rotational bedding need to be derived. The idea is to idealise the profile soil interaction with a rotational bedding spring $c_\vartheta$ and a lateral bedding spring $c_{\mathrm{u}}$, shown in Fig. 1.

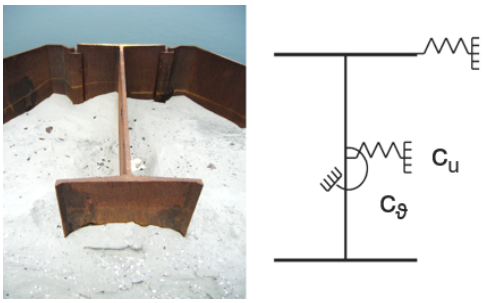


Figure 1: Installed king pile, enclosed by soil (left, Picture done by ArcelorMittal) and simplified system (right)

The rotational bedding of king piles was already investigated within in big field test by [4]. A heavy H-profile was rotated in sand while measuring the moment at the top as well as the rotation over the heigth. Further numerical simulations and back calculations of the rotational bedding during the field tests led to an approach for the rotational bedding of noncohesive soil. As a preliminary study laboratory tests and numerical simulations were performed to analyse the rotational bedding of cohesive soil, as presented.

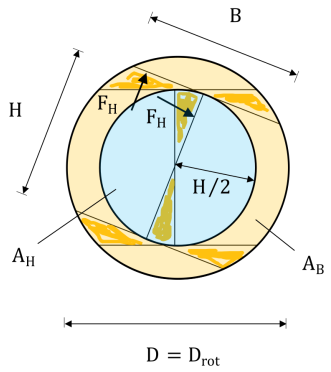


(a)

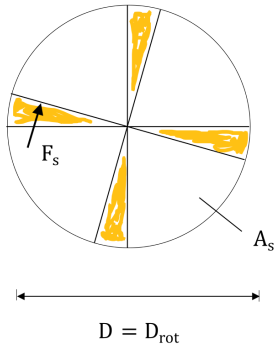


(b)

Figure 2: Shear stress distribution on end face at a positive torque. a) for an H-profile; b) for a standard vane probe

## 3. Laboratory tests

The usage of vane shear tests according to DIN 4094:2002-01,[5] is common practice to determine the undrained cohesion of soil through a correlation between the measured shear resistance moment. For that purpose, wings are rotated in sample whereby the shear resistance of the two circular areas (top and bottom) are measured. Consider an H-formed profile rotated in soil, the areas of resistance will be different but there is still a circular body of rotated soil, as shown in Fig. 2. If the width $B$ gets smaller, a lower geometry ratio $B/H$ follows and the area of resistance gets smaller for small torsion angles. Based on the design of a vane shear test, six different profiles with the same length $L = 50\,\text{mm}$ but different geometry ratio were performed (see table 1). The profiles *H015 - H178* were built by welding plates together and the profiles *H200* as well as *H230* were laser eroded out of a 50 mm thick steel plate. These profiles correspond to the real profiles HZ 680M LT and HP 400x231 scaled by 1 : 20. For the tested soil a clay called "Moorburg Clay" obtained from a stockpile in the harbour of Hamburg Moorburg was used. The Clay was artifically conditioned by homogenizing it and adding water to create three different samples of consistencies: "small (S)" (pulpy, $I_c = 0,47$, $w = 37,3\,\%$), "medium (M)" (soft, $I_c = 0,68$, $w = 32,2\,\%$), "large (L)" (stiff, $I_c = 0,80$, $w = 29,1\,\%$). Next to the geometry and consistency the velocity of torsion $\omega$ was varied between 0,0167 °/s ("V01"), 0,1 °/s ("V06") and 1,0 °/s ("V30"). This led to 36 tests by using the profiles *H015 - H178*. The two others were used to check the derived approach for the rotational bedding. The rotation as well as the measurement of the torsion and moment were performed by a laboratory shear vane test device. The test configuration is shown in Fig. 3.

Table 1: Used model profiles

| name | *H230* | *H200* | *H178* | *H087* | *H060* | *H015* |
|---|---|---|---|---|---|---|
| $D_{rot}$ | 38,0 mm | 27,0 mm | 25 mm | 19,6 mm | 18,6 mm | 17,6 mm |
| $t_f$ | 1,35 mm | 1,30 mm | 1,5 mm | 1,5 mm | 1,5 mm | – |
| $t_w$ | 1,35 mm | 1,30 mm | 1,5 mm | 1,5 mm | 1,5 mm | 1,5 mm |
| $H$ | 30,0 mm | 20,0 mm | 17,8 mm | 17,8 mm | 17,8 mm | 17,6 mm |
| $B$ | 23,0 mm | 20,0 mm | 17,8 mm | 8,7 mm | 6,0 mm | 1,5 mm |

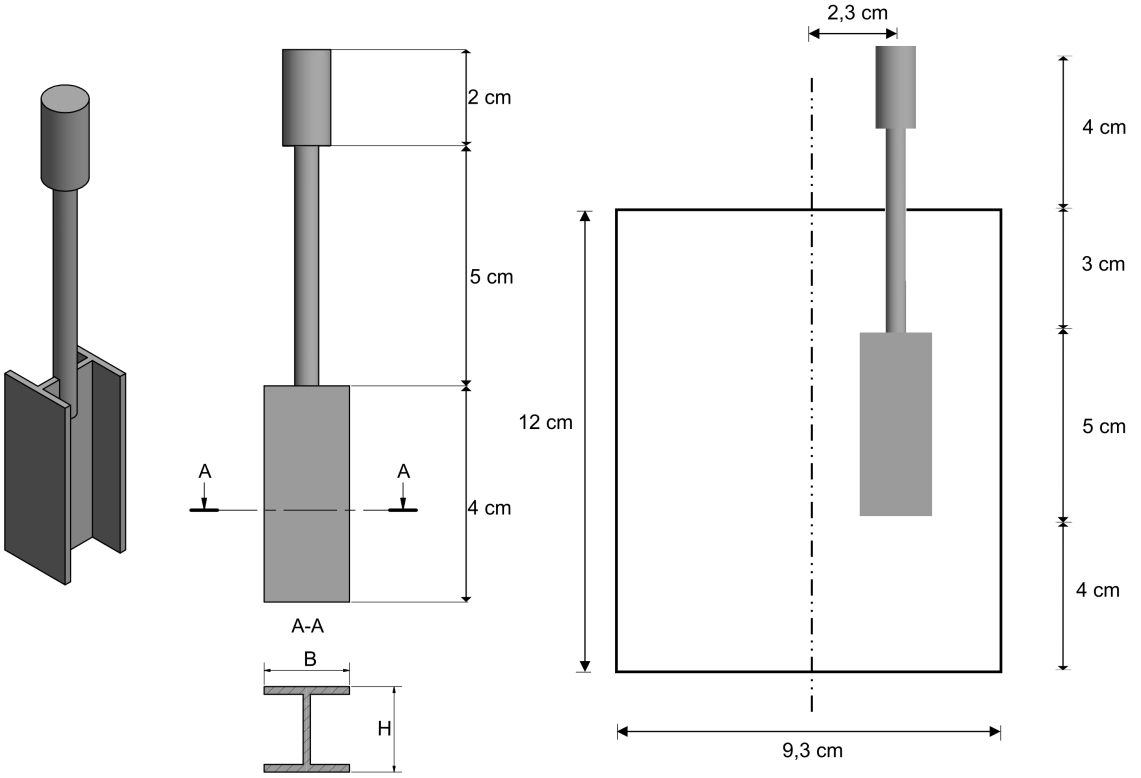


Figure 3: Drawing of a scaled profile used for the rotational stiffness tests with different profile height $H$ and width $B$ (left) and the model profile installed in the sample container (right)

## 4. Results

Firstly it was concluded that the shear resistance grew during the mobilisation of the shear strength. Further torsion ($\vartheta > 20\,^\circ$) did not lead to higher moments $M_\mathrm{T}$ as shown for the variation in the pulpy clay in Fig. 4. To calculate the rotational bedding $c_m$ as bedding over the profile length, the measured moment $M_T$ was divided by the profile length $L$. The result was the line torque $m_T$. The gradients of the torsion line torque graphs found using equation 11 were used to find the rotational bedding $c_m$ for a torsion of $\vartheta = 2\,^\circ$.

$$c_m = \left.\frac{\Delta m_T(\vartheta)}{\Delta\vartheta}\right|_{\vartheta=2^\circ} = \frac{\Delta m_T\,(\vartheta = 2^\circ)}{3,491 \cdot 10^{-2}\mathrm{rad}} \tag{11}$$

The variation of the profile geometry resulted in a linear growth of the rotational bedding for an increasing geometry ratio $B/H$ as seen in Fig. 5 for the soft clay. This behavior was explained by the growing shear resistance areas with respect to the growing diameter $D_\mathrm{rot}$ (cg. Fig. 2a).

Further variation of the consistency showed that the rotational bedding grew exponentially over the increasing consistency number $I_C$. This behaviour is similar to the exponential growth of the undrained cohesion of soil known from the vane shear tests.

Unexpectedly, the variation of the torsion velocity did not lead to a change in the rotational bedding. This behaviour was due to the origin of the clay and the artificial preparation of the sample material. For untouched soil samples of young cohesive soil, the rotational bedding is expected to grow with increasing torsional velocity. A longer consolidation duration might also have led to this expected effect, but was not possible because of the evaporation of pore water.

Neglecting the influence of the profile torsion itself, the growing soil stress over the depth and the torsion speed, a well suiting approach was derived to describe the rotational bedding with

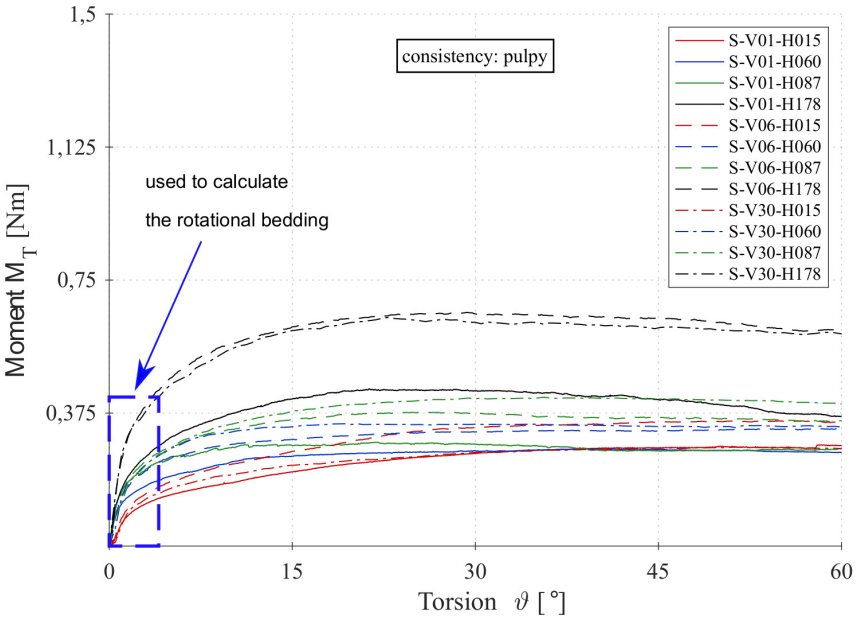


Figure 4: Twisting torque curves of the laboratory tests on the pulpy "Moorburg clay". Range of twisting: 0 to 60 °

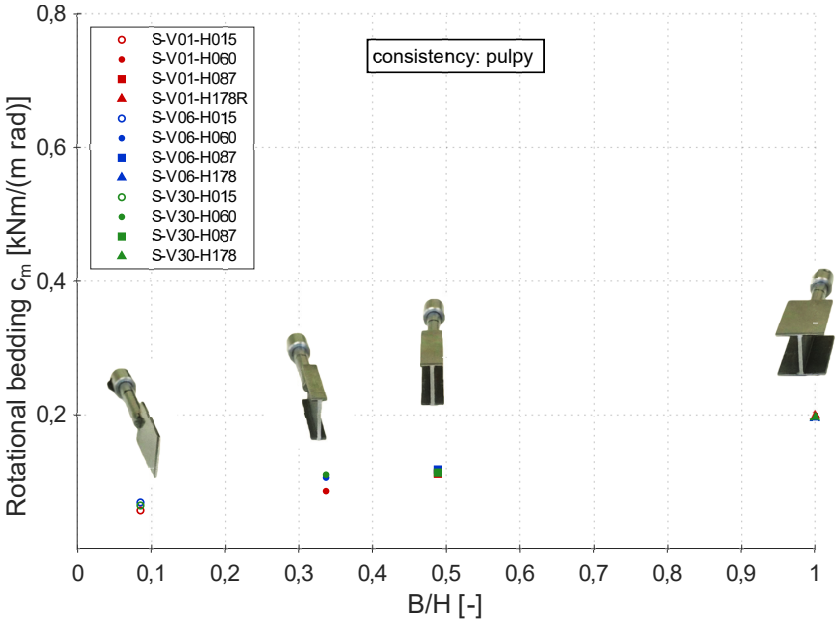


Figure 5: Rotational bedding as a function of the geometry ratio $B/H$ for the laboratory tests on the mushy "Moorburg clay"

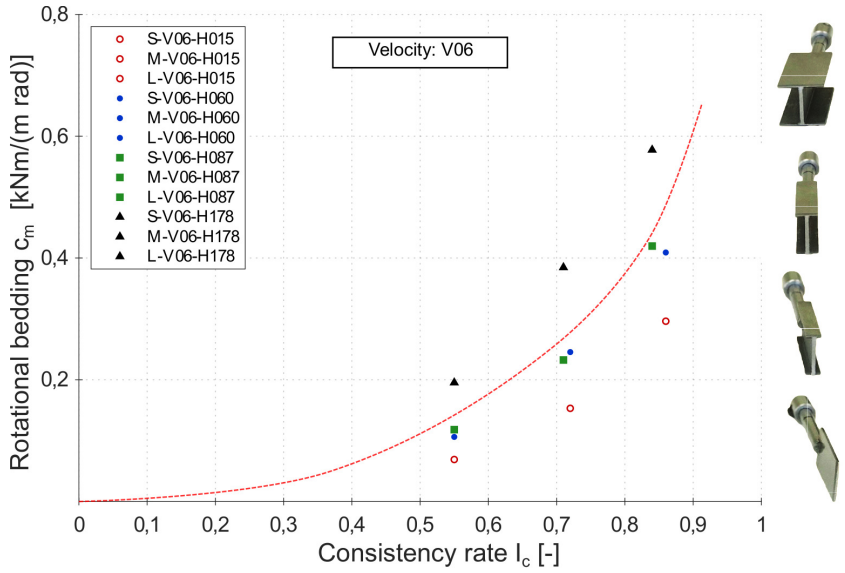


Figure 6: Rotational bedding as a function of the consistency rate $I_c$ for tests with a rotational speed of $0.1\,°/s$

respect of the geometry ratio $B/H$ and the consistency rate $I_c$. Equation 12 was derived by use of a separation approach of the individually varied parameters.

$$\begin{aligned} c_m &\approx c_{m,g}\left(\frac{B}{H}, I_c\right) \\ &= U_{m,g} \cdot \left(a_{g,BH} \cdot \left(\frac{B}{H}\right) + b_{g,BH}\right) \cdot \left(a_{g,Ic} \cdot \sin\left(I_c - \pi\right) + b_{g,Ic} \cdot \left(I_c - 10\right)^2 + c_{g,I_c}\right) \end{aligned} \tag{12}$$

with

$$U_{m,g} = \frac{1}{0,4657} \frac{\mathrm{m \cdot rad}}{c_{m,g}\left(\frac{B}{H} = 0,489, I_c = 0,85\right)}$$

$$a_{g,BH} = 0,3390 \frac{\mathrm{kNm}}{\mathrm{m \cdot rad}} \qquad b_{g,BH} = 0,2934 \frac{\mathrm{kNm}}{\mathrm{m \cdot rad}}$$

$$a_{g,l_c} = 6,4586 \frac{\mathrm{kNm}}{\mathrm{m \cdot rad}} \qquad b_{g,I_c} = -0,3263 \frac{\mathrm{kNm}}{\mathrm{m \cdot rad}} \qquad c_{g,I_c} = 32,6265 \frac{\mathrm{kNm}}{\mathrm{m \cdot rad}}$$

## 5. Further investigation

With the knowledge that the laboratory tests were not able to adequately represent the real conditions, further investigations are still necessary. As such, numerical simulations of the rotation of different profiles in cohesive soils were performed. For a meaningful validation of the numerical simulations a field test with real dimensions is required. For that purpose a real king pile is planned to be rotated next to a quay wall in the natural clay layer to derive the rotational bedding (cf. Fig. 7) as was done in sand by [4].

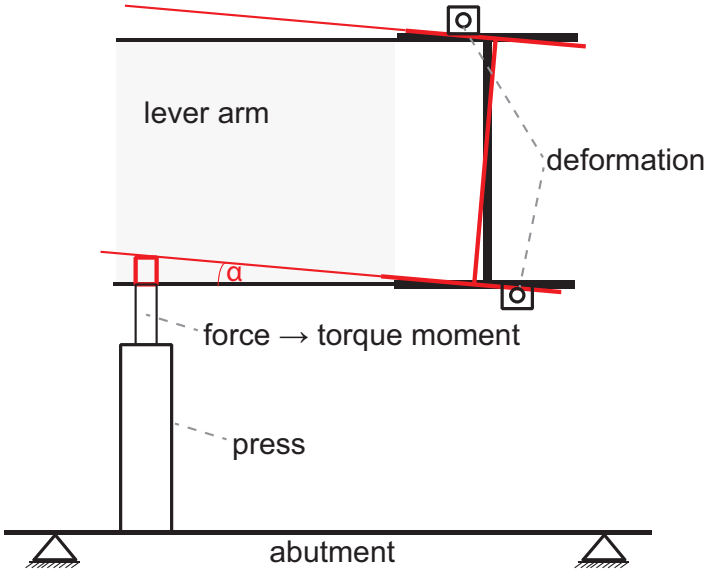


Figure 7: Torsion of a king pile by use of a lever arm and a cylinder press

For investigation of the reactional pressure caused by the rotation of the profile, combined earth and water pressure sensors are going to be installed on the web of the profile in three levels. Further the deformation is measured in the external axes by chain inclinometer probes to calculate a rotation of the profile. Therefore, a back calculation of the rotational bedding is possible due to measurement of the reaction moment at the top of the profile (see construction drawing in Fig. 8).

As expected that the rotational bedding in cohesive soil, especially young clay, is much lower than in sand, an additional test is planned. After having done the test in the clay the profile shall be installed additional in the lower sand layer as it would be done in reality. That is how the impact of the rotational bedding in cohesive soil compared to the rotational bedding in noncohesive soil shall be derived.

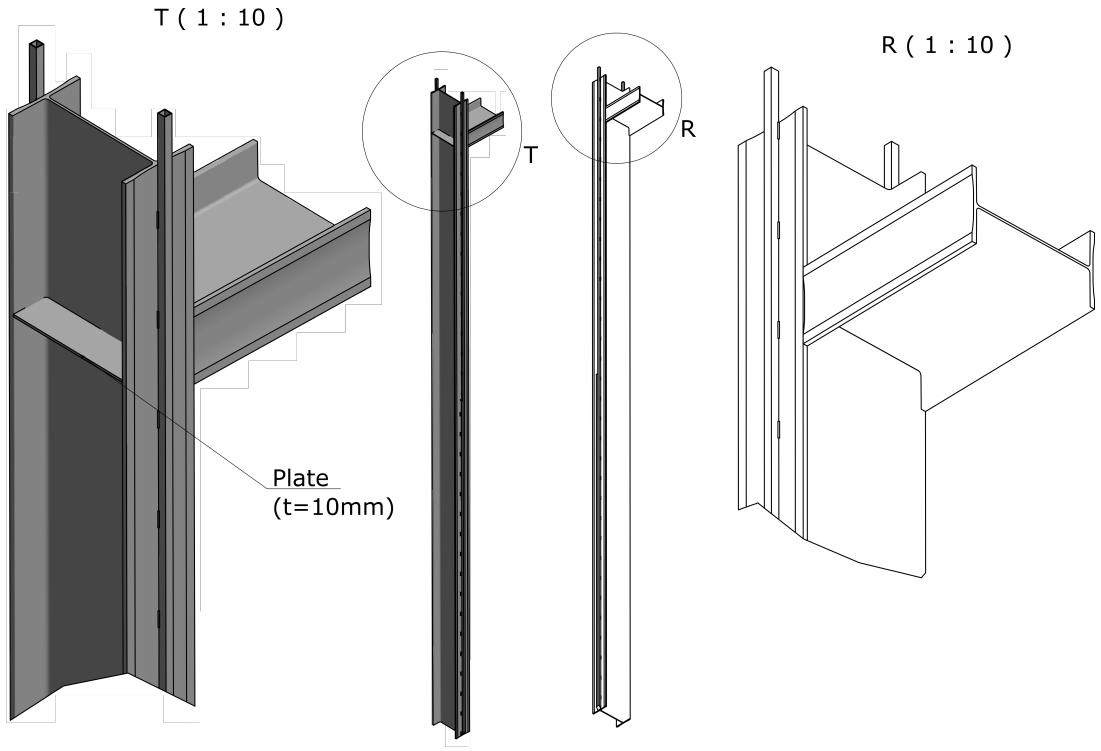


Figure 8: Drawing of the test pile for the rotational bedding test

## 6. Concluding Remarks

As a result of the high loads which cause normal forces and bending moments, the stability of the king piles of combined sheet pile walls is endangered. Due to the introduction of the standards of DIN EN 1993-5:2010-12 [1] in connection with DIN EN 1993-1-1:2010-12 [2] the proofing of combined walls needs to be done under combination of the resistance against flexural buckling and lateral-torsional buckling. For that reason the rotational resistance of the soil must be considered in order to ensure an economical design.

For construction building, the verification against torsional flexural buckling of beams can be done by taking stiffening elements such as adjoining components or trapezoidal sheets on purlins into account. That is done be idealisation of the stiffening by a continuously rotating spring $c_\vartheta$ or by a single spring $C_\vartheta$ [3]. This consideration leads to a higher acceptable moment of the profile. The aim was to transfer this approach to geotechnical problems. For that purpose a back calculation for the rotational bedding of an H-profile in sand was done by [4] and showed that the use of an additional rotational bedding led to higher safety factors for the verification against torsional flexural buckling. The rotational bedding in cohesive soil is different from that in noncohesive soil and was investigated by laboratory tests as well as by numerical simulations. Laboratory tests were performed to explore the dependency of the rotational bedding in cohesive soil. For that purpose six model profiles with a length of 50 mm were created by a varying geometry ratio $B/H$ from 0.08 to 1.00. For soil, a clay called "Moorburg Clay" obtained from a stockpile in the harbour of Hamburg in a pulpy, soft and stiff consistency. Next to the geometry and consistency the velocity of torsion $\omega$ was varied between 0,0167 °/s and 1,0 °/s.

The profiles were drilled in a vane shear test device to calculate the rotational bedding backwards from the torsion and the measured moment at the top of the profiles. As result the variation of the geometry showed that the rotational bedding increased nearly linearly with increasing geometry ratio $B/H$. Further, the rotational bedding grew nearly exponentially with increasing consistency rate. Using a separation approach, equation 12 gave an accurate approximation for the laboratory tests with respect of neglecting the rotation speed.

Further investigations using real scale field tests as well as numerical simulations are planned to derive an approach for the rotational bedding that is suitable for real sized king piles in soil.

## 7. Acknowledgements

The IGF project 19937 / 1327 "Optimized design of combined steel sheet pile walls for the installation process and the final state" of FOSTA - Forschungsvereinigung Stahlanwendung e. V., Düsseldorf, is funded via the AiF within the framework of the programme for the funding of joint industrial research (IGF) by the Federal Ministry of Economics and Energy on the basis of a resolution of the German Bundestag. The project is carried out at the Institute of Geotechnical Engineering and Construction Management (TU Hamburg) and the Institute of Construction and Design (University of Stuttgart). We would like to thank the members of the Project supporting Committee of the project for their participation.

## References

[1] DIN EN 1993-5 2010 *Eurocode 3: Bemessung und Konstruktion von Stahlbauten – Teil 5: Pfaehle und Spundwände* (Beuth Verlag GmbH)
[2] DIN EN 1993-1-1 2010 *Eurocode 3: Bemessung und Konstruktion von Stahlbauten – Teil 1-1: Allgemeine Bemessungsregeln und Regeln für den Hochbau* (Beuth Verlag GmbH)
[3] Lohse W, Laumann J and Wolf C 2016 *Stahlbau 1: Bemessung von stahlbauten nach eurocode mit zahlreichen beispielen* (Springer-Verlag)
[4] Schallück C and Grabe J 2011 *Tagungsband zum Workshop Ports for Container Ships of Future Generations, Veröffentlichungen des Instituts für Geotechnik und Baubetrieb der TU Hamburg-Harburg, Heft 22* pp 329–344
[5] DIN 4094 2002 *Baugrund – Felduntersuchungen – Teil 4: Fluegelscherversuche* (Beuth Verlag GmbH)